The American Journal of Human Genetics, Volume *102*

Supplemental Data

Impaired Transferrin Receptor Palmitoylation and Recycling in Neurodegeneration with Brain Iron Accumulation

Anthony Drecourt, Joël Babdor, Michael Dussiot, Floriane Petit, Nicolas Goudin, Meriem Garfa-Traoré, Florence Habarou, Christine Bole-Feysot, Patrick Nitschké, Chris Ottolenghi, Metodi D. Metodiev, Valérie Serre, Isabelle Desguerre, Nathalie Boddaert, Olivier Hermine, Arnold Munnich, and Agnès Rötig

Figure S1. Quantification of steady-state levels of proteins involved in iron homeostasis.

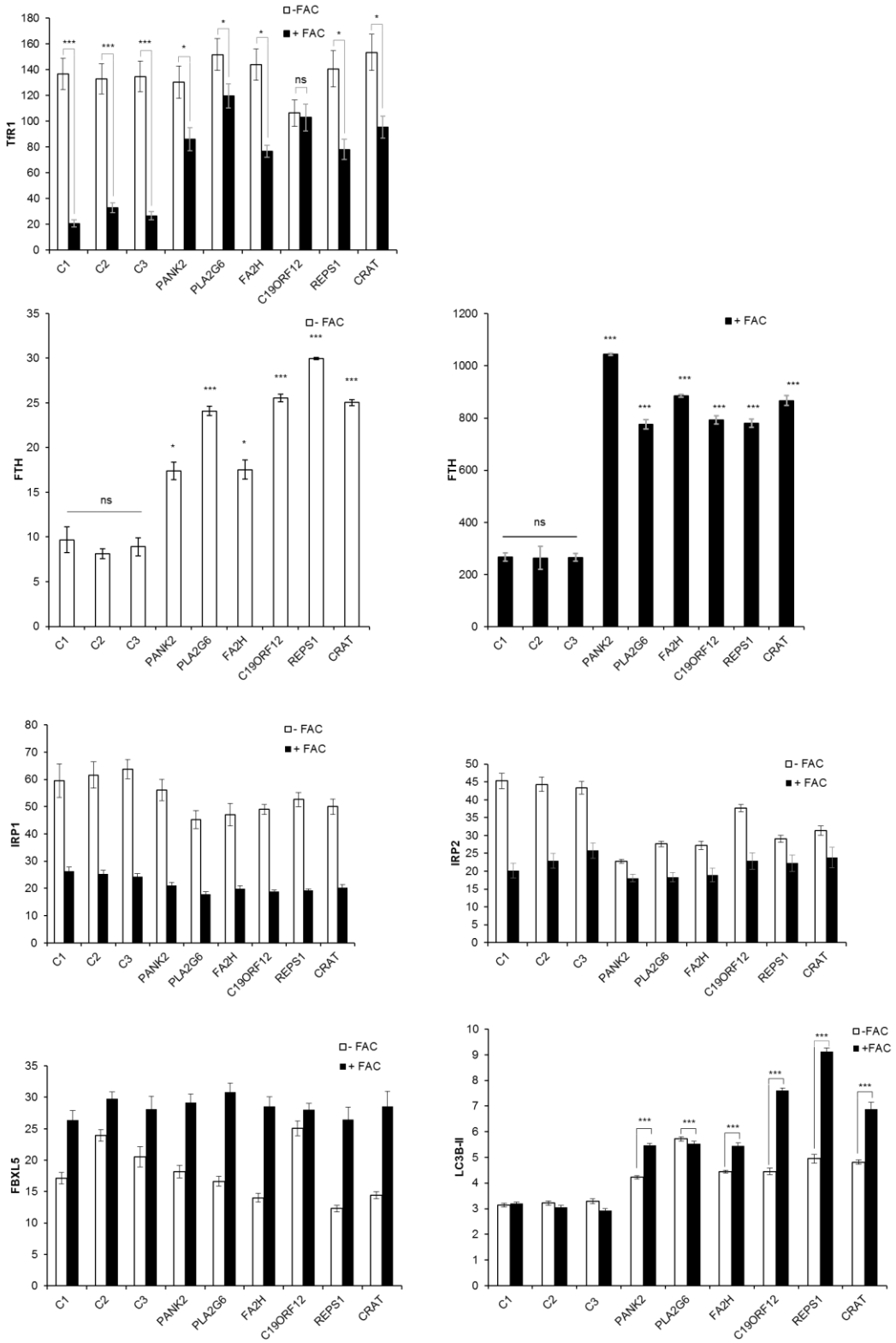

Immunoblotting quantification of steady-state levels of proteins involved in iron homeostasis in low (-FAC) and high iron conditions (+FAC) presented in Figure 3. TfR1, FTH, IRP1, IRP2, FBXL5 and LC3B amounts are relative to actin. The data are the means ± SEM of three independent experiments. C1-3: control fibroblasts. TfR1 Paired sample t-test (TfR1) or One Way Analysis Holm-Sidak method (ferritin) were used. * and *** correspond to *P* values <0.05 and <0.001 respectively, ns: non-significant.

Figure S2. Quantification of steady state levels of proteins presented in Figure 7.

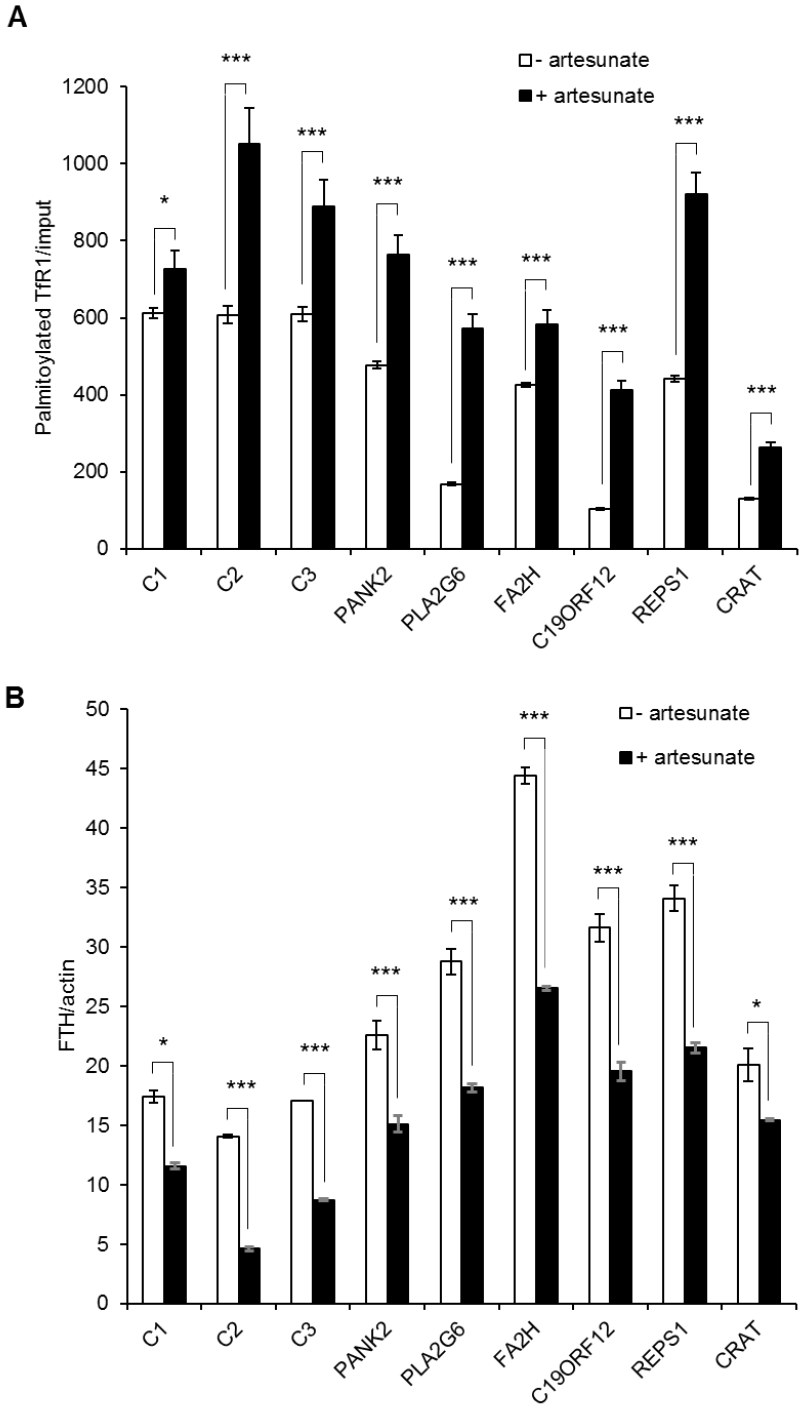

A. Quantification of TfR1 palmitoylation in fibroblasts of controls and NBIA subjects. **B**. Quantification of ferritin in fibroblasts treated or not with 25 µM artesunate. The data are the means ± SEM of three independent experiments. C1-3: control fibroblasts. Paired sample t-test (TfR1) or One Way Analysis Holm-Sidak method (ferritin) were used. * and *** correspond to *P* values <0.05 and <0.001 respectively, ns: non-significant.

Figure S3. Iron content and regulation of iron homeostasis in fibroblasts of NBIA subjects.

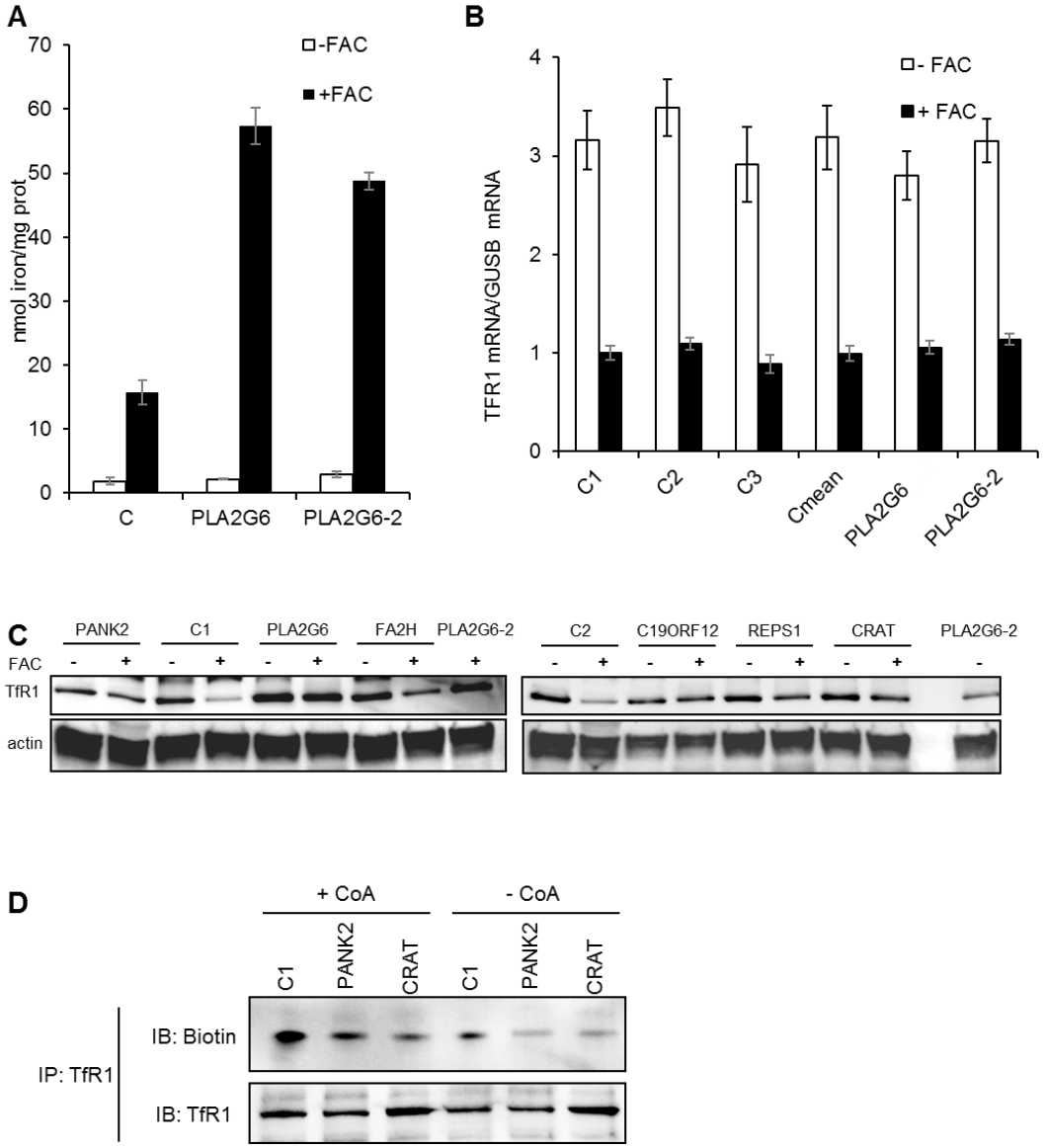

A. Iron quantification using the ferrozine-based colorimetric assay in fibroblasts of controls (C, mean of 3 controls) and two PLA2G6 subjects (PLA2G6, already presented in other figures, and PLA2G6-2) grown in FBS-free DMEM medium and low (-FAC) or high iron conditions (+FAC). The data are the means ± SEM of three independent experiments. Student-Newman-Keuls ANOVA multifactorial test was used. **B.** Post-transcriptional regulation of iron homeostasis in fibroblasts of controls and two PLA2G6 subjects grown in FBS-free DMEM medium in low (-FAC) or high iron conditions (+FAC). *TFRC* mRNAs were quantified by ddPCR and expressed as a ratio to *GUSB* mRNA. The data are the means ± SEM of three independent experiments. The significance of variations among samples and controls was estimated using One Way Analysis Holm-Sidak method. **C.** Steady-state levels of TfR1 studied in non-reducing conditions (7.5% acrylamide, no dithiothreitol (DTT), no heat denaturation) in fibroblasts of controls (C1-2) and NBIA subjects grown in FBS-free DMEM medium in low (-FAC) and high iron conditions (+FAC). Actin was used as loading control. **D.** Effect of CoA supplementation on TfR1 palmitoylation in PANK2 and CRAT-deficient fibroblasts. Fibroblasts were treated with or without CoA 25 µM for 72 h, and TfR1 protein was immunoprecipitated with mouse anti-TfR1 antibody to perform the palmitoylation assay. In each condition, the upper panel shows the palmitoylated TfR1 level (IB: Biotin) and the immunoprecipitated amount of TfR1 (IB: TfR1).

Figure S4. Brain MRI of subjects 1-3.

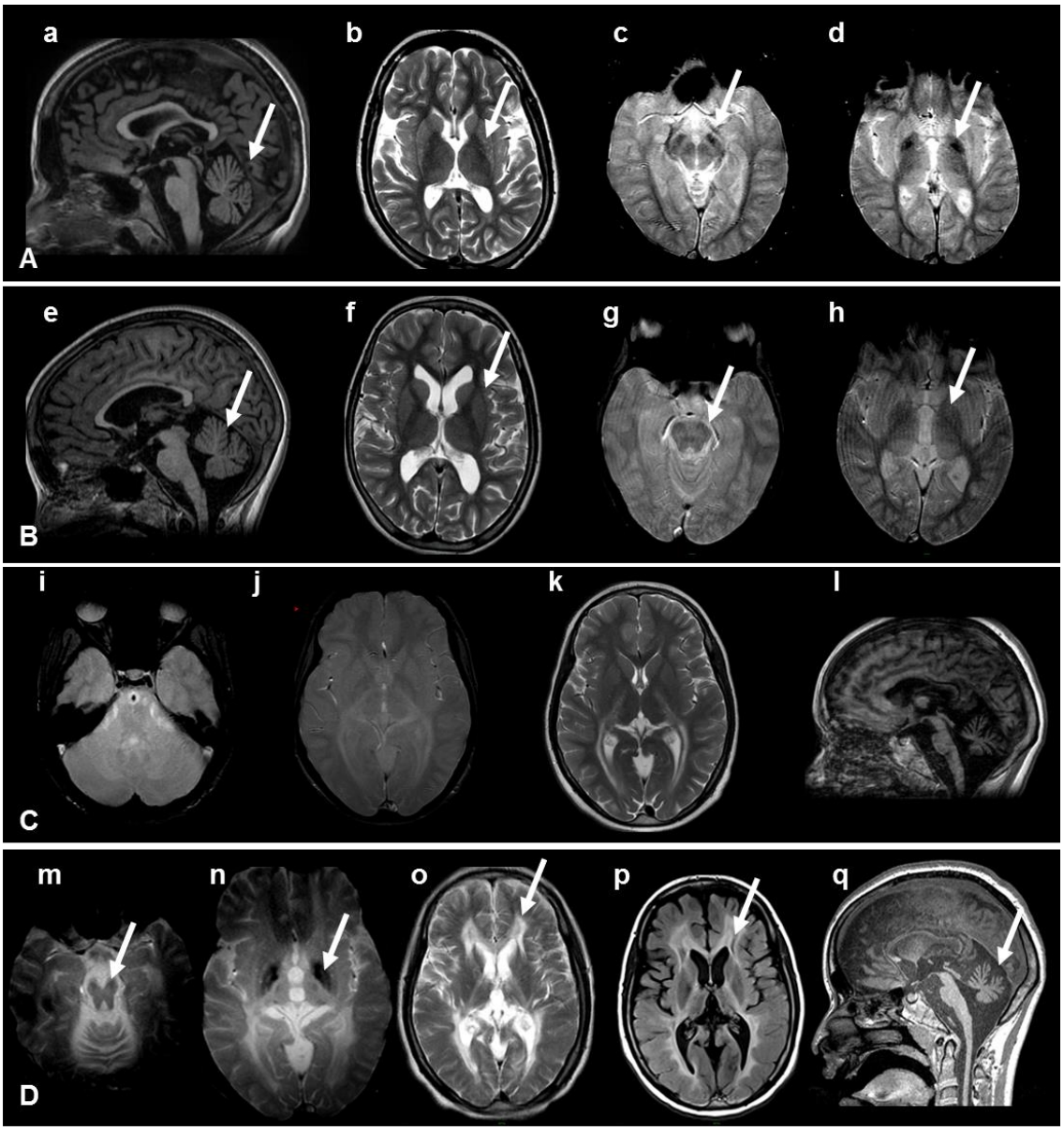

A. Brain MRI of subject 1 at 15 yr of age. Moderate cerebellar atrophy and thinning of the corpus callosum is seen on sagittal T1 (a). Putamen and caudate nuclei hyperintensity is seen on the T2 weighted image (b; arrow). Hypointensity of the substantia nigra (c) and globus pallidus (d) consistent with iron deposition, is seen on axial T2* (arrows). **B.** Brain MRI of subject 2 at 10 yr of age. Moderate cerebellar atrophy and thinning of the corpus callosum is seen on sagittal T1 (e, arrow). Neither basal ganglia anomalies on T2 weighted images (f; arrow) nor hypointensity of the substantia nigra (g) or globus pallidus (h) are seen on axial T2* (arrows). **C.** Brain MRI of subject 3 at 10.8 yr of age. No hypointensity of the substantia nigra (i) and globus pallidus (j) was seen on axial T2*. White matter hyperintensity is only seen in the posterior arm of the internal capsule on the T2 weighted image (k). Profound cerebellar atrophy and thinning of the corpus callosum is visible on sagittal T1 (l). **D.** Brain MRI of subject 3 at 15.5 yr of age. Hypointensity of the substantia nigra (m) and globus pallidus (n) consistent with iron deposition is seen on axial T2* (arrow heads). White matter hyperintensity is shown as well (o and p; arrows), with features of a necrotizing leukoencephalopathy evident on axial Flair weighted images (p). Profound cerebellar atrophy and thinning of the corpus callosum is also evident on sagittal T1 (q).

Table S2. Sequences of primers used for ddPCR

Primer	Sequence
TFCR	5′-gctgcaggttcttctgtgtggca-3′
TFRC reverse	5′-cgagccaggctgaaccgggta-3′
GUSB forward	5′-gcggtcgtgatgtggtctgt-3′
GUSB reverse	5′-gtgagcgatcaccatcttcaagt-3′

Primers were designed using the Oligo Primer Analysis Software v.7 available at http://www.oligo.net. The specificity of primer pairs to PCR template sequences was checked against the NCBI database using the Primer-BLAST software (http://www.ncbi.nlm.nih.gov.gate2.inist.fr/tools/primer-blast).

Supplemental Note: Case reports

Subjects

Subject 1, the third child of unrelated healthy parents of French origin (birth weight: 2.6 Kg, height: 46.5 cm, OFC: 33.5 cm) had speech and motor delay. She did well during the first few months and walked alone aged 18 mths but her speech was delayed and she developed trunk hypotonia, progressive cerebellar ataxia, pyramidal syndrome for unknown reasons and lost the ability to walk at age 9 yrs. At this same age, nystagmus, dysarthria, dysmetry, spasticity of the lower limbs and *pes cavus* were noted. Skeletal muscle biopsy revealed negative SDH and COX staining in numerous fibers, but plasma lactate, pyruvate, amino acids and very long chain fatty acids were unremarkable and mitochondrial respiratory chain enzyme activities were normal. Brain MRI showed progressive cerebellar and cerebral atrophy and T2* evidence of brain iron accumulation in the *globus pallidi* and peduncles (Supplementary Figure 4). She gradually lost the ability to walk and stand unaided then to hold her head at 14 yrs. Swallowing difficulties, stiffness of the limbs, severe dystonia and nystagmus appeared. She died aged 20 yrs after a 10-yr gradual worsening of her condition.

Subject 2, the sister of subject 1, had a similar, albeit slightly milder clinical course. Aged 14 yrs, she can still walk with aids, hold a pencil and practice indoor bike and swimming. Interestingly, the parents mentioned some fluctuations in their neurological conditions and a significant worsening following monthly menstruations in subjects 1-2.

Subject 3, a girl born to first cousin Turkish parents after a term pregnancy and normal delivery (birth weight: 3.5 Kg, height: 51 cm, OFC: 35 cm) walked at age 14 mths but exhibited a speech delay first ascribed to a mild hearing loss. Unbalanced gait and slowly progressive cerebellar ataxia were noted at 3 yrs. She gradually lost the ability to stand, walk and write. Tremor, dysmetry, hypotonia, brisk deep tendon reflexes and sensory neuropathy were suggestive of slowly progressive spinocerebellar degeneration. Extensive metabolic workup showed normal plama lactate, pyruvate and amino acids. Interestingly, absolute concentrations of very long chain fatty acids in plasma and their molar ratios were elevated, compared to controls (C22:48.6 µmol/L, normal: 21-46; C24: 63.7 µmol/L, normal: 22-49; C24/C22: 1.3, normal ± 1SD: 0.86±0.07). Normal respiratory chain activities were observed in muscle, liver and fibroblasts. Brain MRI showed evidence of cerebellar atrophy and posterior leukodystrophy. Hyperintensity of basal ganglia and hypointensity of *globus pallidi* and *substantia nigra* on T2* sequences were suggestive of major iron accumulation (Supplementary Figure 4).